A 1.5D transducer for medical ultrasound

C.M.W. Daft, D.G. Wildes, L.J. Thomas, L.S. Smith, R.S. Lewandowski, W.M. Leue, K.W. Rigby, C.L. Chalek and W.T. Hatfield.

GE Corporate R&D, Schenectady, NY 12301-0008.

1 Abstract

The current shift to digital beamforming technology holds promise for regular and rapid increases in the number of channels in a medical imager. A 1D transducer typically utilizes 128 elements, while a fully sampled two-dimensional aperture requires of order 10000 elements. Currently, channels are still expensive, so it is of interest to evaluate how much performance can be improved with a moderate increment in channel count. How may we maximize the impact on voxel size? The number of elevational elements is constrained by how complex the interconnections can become. It is impractical to significantly degrade the azimuthal resolution from the 1D case.

We present beam profiles and images from a first attempt at judicious use of a 256 channel imager. Simulations and experiments allow us to explore compromises among a number of design goals. We have fabricated a transducer with several elevational rows which reduces the slice thickness of the image while maintaining full azimuthal resolution.

2 Digital beamforming and 1.5D arrays

This work was performed using a GE LOGIQ 700 imager, which uses a digital beamformer to provide higher precision image reconstruction than is possible with analog electronics. Digital beamforming is useful for several other reasons: first, there is an inherent advantage in scaling to larger numbers of channels. With an analog beamformer, the number of delay lines required increases as the square of the number of channels, assuming that the array consists of a linear sequence of elements. This is because the required steering delays per channel are linear in array size, while the number of channels is also increasing with array size. In a digital beamformer, the number of components does not need to increase with increasing delay requirements. Thus, we expect the cost per channel to decrease relative to analog beamformers as channel counts inexorably increase.

Also, digital beamformers tend to provide uniformity over a full range of transducer frequencies, while analog beamformers are only optimal for a restricted frequency range. We have further found that the requirements of phase and time delay accuracy increase severely as the array grows larger in wavelengths. It's much easier to maintain a desired accuracy with a digital beamformer. We can also add advanced features, such as two-for-one frame rate increases [1] and imaging of solids for NDE with little additional expense.

With a digital beamformer, we can control channels autonomously. In contrast with analog imagers, we need make no assumptions about the locations of transducer elements. Consequently, we can image with two-dimensional arrays with relative ease [2]. The transducers we will discuss in this paper have small numbers of elements in elevation, and so are termed "1.5D" arrays.

In this paper, our 256 channel imager is tested with a 1.5D array in an effort to improve upon the fixed elevational lens focus by adding dynamic focusing in elevation. The goal is to provide images of thinner slices of the body through control of the elevational beam profile. Figure 1 shows the different options which become available with an increased number of channels.

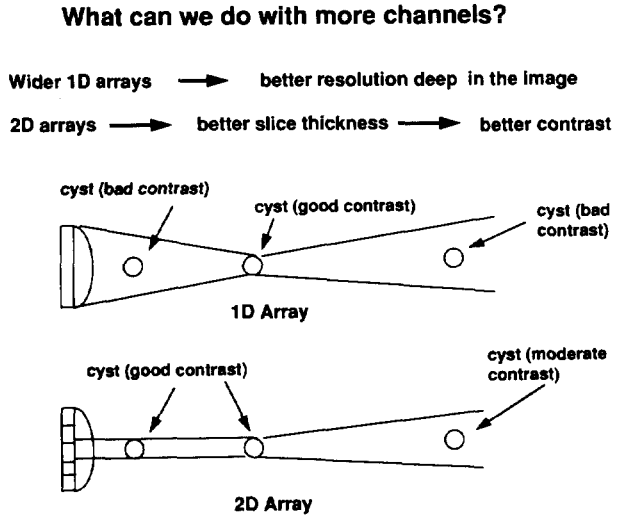

Figure 1.

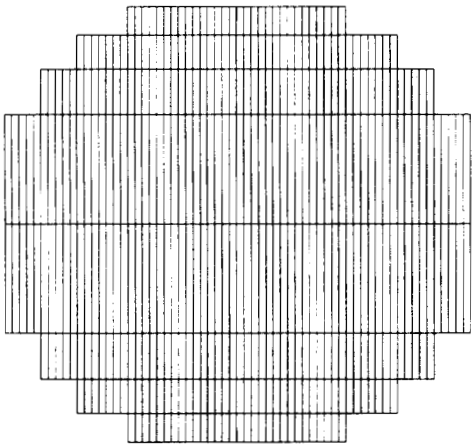

Figure 2: outline of a 7 row 1.5D array. Scanning is only performed in the well-sampled direction (horizontally).

3 Optimizing the transducer

Figure 2 shows the type of 1.5D array we considered for this project. Several points should be made about this drawing. First, there are many elements in azimuth (X). This is so that the array performs similarly to standard 1D transducers in resolution and penetration. The elements in elevation (Y) are much wider and fewer in number. This makes it impractical to steer in elevation, due to the grating lobes from the undersampled elevational aperture. Such an array will also continue to require a lens in elevation. The lens allows a helpful variation of phase across the element, which we cannot achieve with the beamformer.

Tradeoffs abound in the design of a 1.5D array, because the total number of elements is fixed. Not only must we decide on the relative importance of azimuth and elevation resolution, near field and far field performance are also important. For good near field imaging, it's important that the central elements be small, so the aperture can be reduced. In the far field, the important point is how well the effect of the lens can be cancelled. This calls for a Fresnel lens arrangement in which the boundaries of the elevational elements are proportional to the square root of the row number. This relation arises from the quadratic dependence (to first order) of focusing time delay on position in the aperture. The corner elements are not present, to conserve channels. The beam profile of a circular array is roughly a Bessel function, while the beam profile of a square array approximates a product of sinc functions. The corner elements are thus the least painful to remove because we gain some reduction in sidelobe level at the cost of detail resolution.

Figure 3 indicates the effects of different numbers of elevational rows on the resolution. The resolution at -5 dB and -20 dB is plotted for arrays with 1, 3, 5, 7 and 65 elevational rows. In these graphs, low values equate to good resolution. At the lens focus of 57 mm, the transducers are all equal, because the lens is providing perfect beamforming with no supplementation from the beamformer. At smaller ranges, the differentiation between arrays is clear, and reflects the advantages in apodizing the array in elevation.

The improvements in the far field are more complex. At the -5 dB contour, there is little difference between the 3 row array and "perfection". At -20 dB, it becomes clear again that the more rows in the array, the better.

4 A practical 1.5D probe

Figure 4 shows a 1.5D transducer we have constructed to test these simulations. We would like to evaluate the effect of slice thickness improvements on clinical image quality. This probe has a center frequency of 3.75 MHz, and an azimuth resolution equivalent to a 1D sector probe of this frequency. It is built using standard PZT ceramic with a silicone lens, but with a novel interconnect technology. It is not a sparse array [3]: the elements fill the entire aperture. We have carefully balanced the conflicting requirements outlined above to maximize the improvement in voxel size.

5 Measuring beam plots

The experimental setup is illustrated in figure 5. The transmitted signal was produced by a small spherical ball source. We measured the signal produced by this transducer over a range of ± 20 degrees and found it to be highly isotropic (less than 5% variation over this range). The spherical source was fired by a delayed version of the transmit synchronization signal, to mimic the propagation of sound from the array to a reflector. The timing was checked for consistency with the position of the spherical source, which was mounted on a stand with a calibrated screw thread.

We programmed the data acquisition system (a logic analyzer connected to a large memory) to record only the center 20 beams from `LOGIQ 700`. This speeds the data collection, and is possible because we are interested in beam profiles in elevation, and only wish to evaluate the azimuthal beam profile at its peak. 20 beams were found to be adequate for this purpose. After each batch of beams was recorded, the data acquisition PC issued a "bump" command, instructing the motion controller to move to the next elevation. The next portion of a frame was then recorded.

6 Slice thickness improvements

A 3D data set containing range, azimuth and elevation coordinates was acquired for source positions of 30, 80 and 140 mm from the transducer. For comparison, both the 1.5D and 1D transducers were measured under identical conditions.

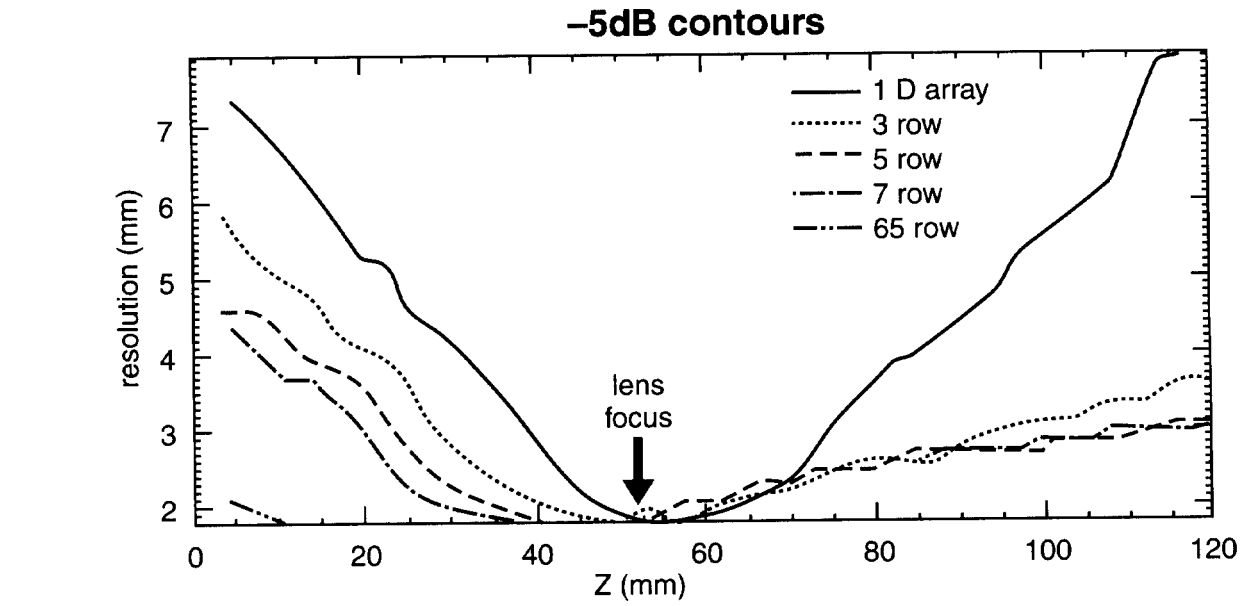

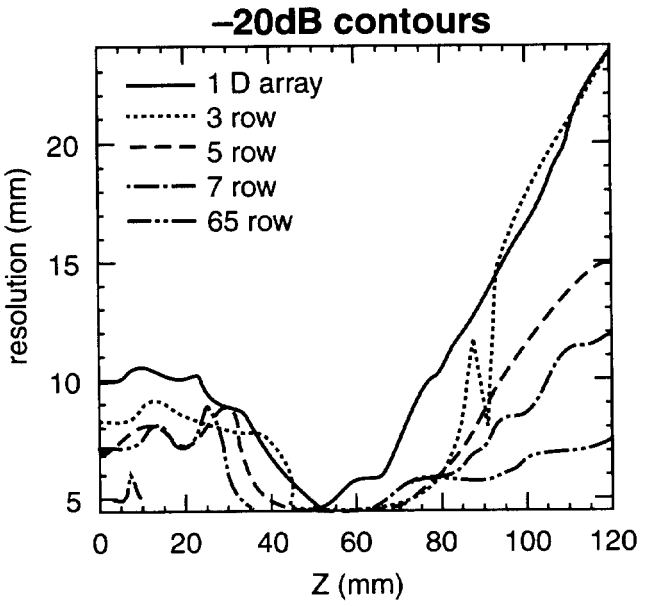

Figure 3: elevational resolution at -5 dB (above) and -20 dB (left) for different aperture complexities.

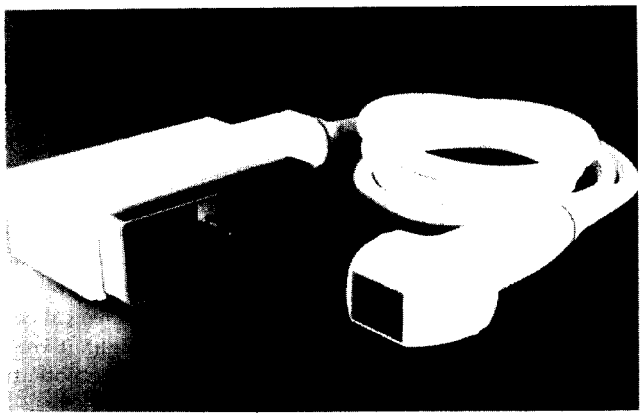

Figure 4: experimental 1.5D transducer.

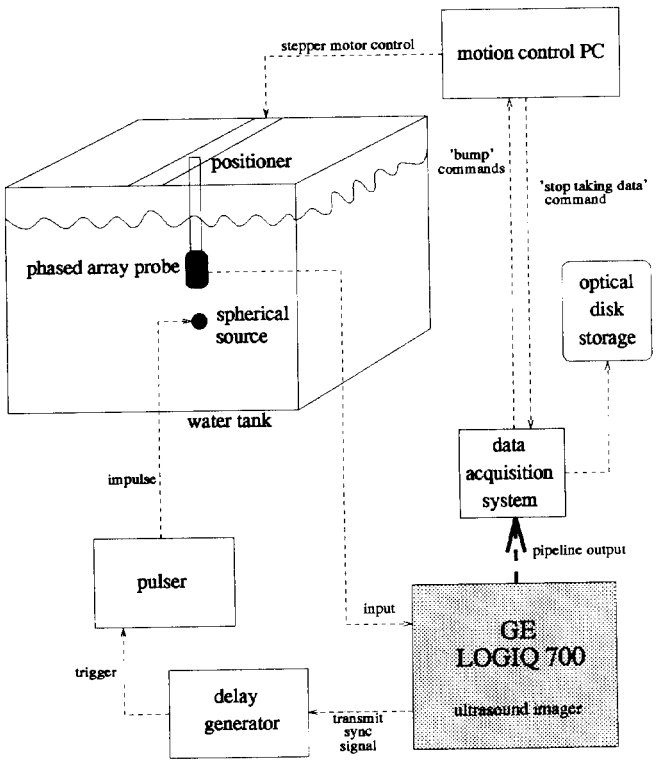

Figure 5: apparatus for measuring resolution.

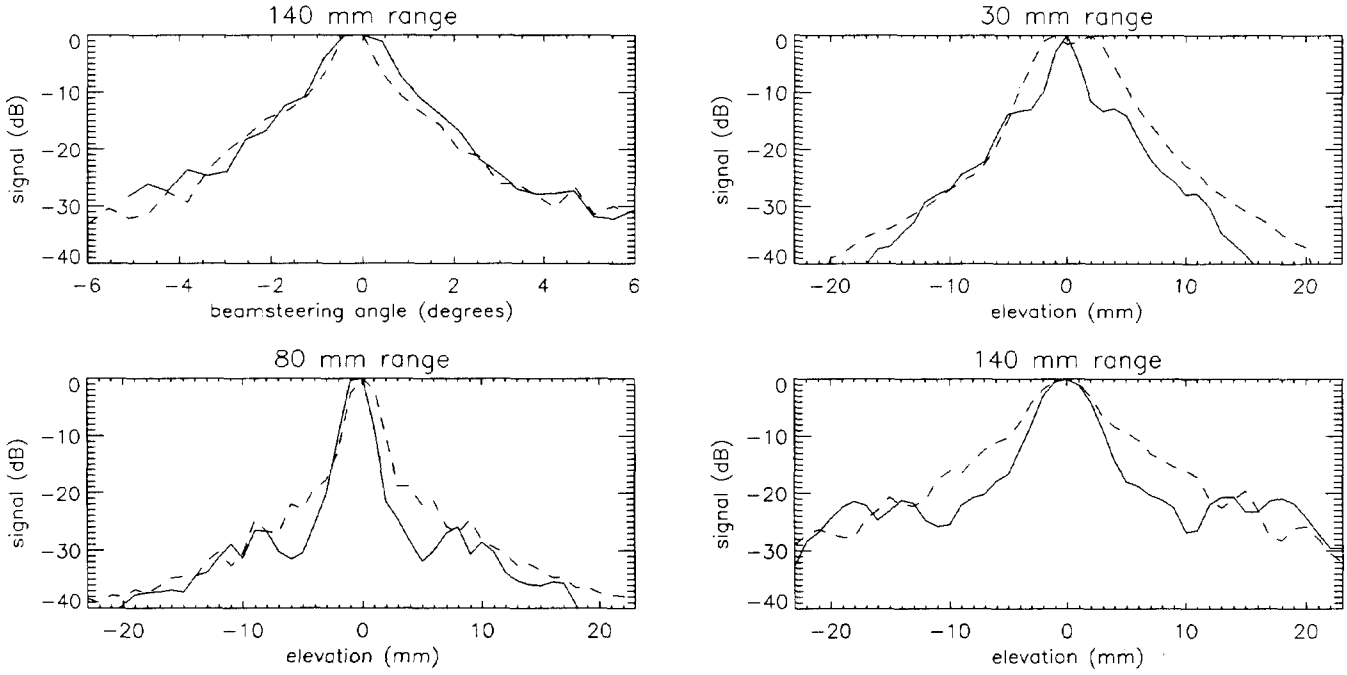

Figure 6: comparison of 1D and 1.5D experimental results: dashed line is 1D, solid line is 1.5D data (see text below).

Figure 6 shows experimental data in which the two arrays are compared. Consider the top left graph. In all of these plots, the 1.5D array data is a solid line, while the 1D data is dashed. The azimuthal resolution at 140 mm is very similar to that measured with the 1D probe. In elevation, the 1.5D array is clearly superior. At 30 mm, the improvement in slice thickness is due to the apodizing of the outer rows. We can maintain a constant F-number in elevation with the 1.5D array, unlike the 1D array where the F-number becomes uncomfortably small close to the transducer. At 80 mm, the 1.5D array is also better. This is caused by its larger elevational aperture, and also the fact that we are apodizing in elevation. At 140 mm, the improvement is due to the focusing of the outer rows. They are effectively nulling out the lens which is focused closer in for both transducers.

7 Phantom and clinical images

Further experiments were conducted on tissue mimicking phantoms and human volunteers. Figure 7 shows the slice thickness improvements in a standard RMI phantom turned at 90 degrees from the normal imaging direction. While useful for measuring contrast and detail resolution in azimuth, phantoms are so large in elevation that their images are not a strong function of slice thickness. However, if the phantom is rotated, the effect of slice thickness on a finite cyst can be observed. In these images, the cysts appear as cylinders being viewed on their long axes. The interesting parts of figure 7 are the degrees of "cystic clearing", i.e., how much the cysts' lack of scattering is captured in the picture. This is a measure of the partial volume effect: if the slice is very thick, we will be imaging the tissue equivalent gel as well as the cyst. This will show up as a diminution of contrast between tissue and cyst. The 1D array and the 1.5D array both show good contrast with the deeper cyst at 60 mm. This is because in the mid range of the image, the lens is beamforming adequately. However, the cysts at 30 mm look very different between the 1D and 1.5D cases. The 1D image lacks cystic clearing, whereas the improved slice thickness of the 1.5D array is obvious.

A pair of scans of the liver in a subject with a hemangioma (a benign tumor made up of new-formed blood vessels) are shown in figure 8. The hemangioma is the circular structure in the images: also visible are the diaphragm, a large vessel, and the margin of the liver. The probe is positioned on the patient's side. The contrast between the hemangioma and the rest of the liver is enhanced in the 1.5D case.

Perhaps even more important than the increased visualization of low contrast objects is the ease with which the unusual anatomy can be found with the 1.5D probe. This particular hemangioma took an experienced radiologist considerable time to find with the 1D probe. The images in figure 8 are the best he could obtain. With the 1.5D probe, producing a superior image requires less skill. The image may also be obtained much more quickly. In the current atmosphere of health care cost containment, the medical community is concerned with issues of patient throughput versus diagnostic accuracy. Thus, 1.5D imaging has the potential to contribute to more economic and accurate diagnoses.

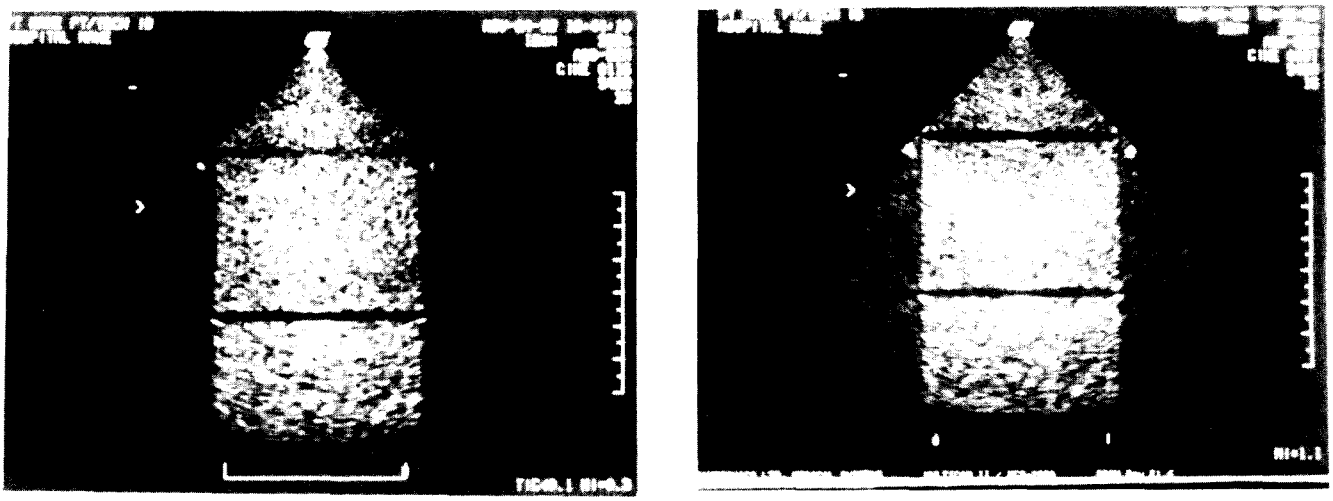

Figure 7: images of phantom rotated 90 degrees with 1D transducer (left) and 1.5D transducer (right). The cystic clearing is much better in the 1.5D array at 30 mm, and is equivalent at 60 mm.

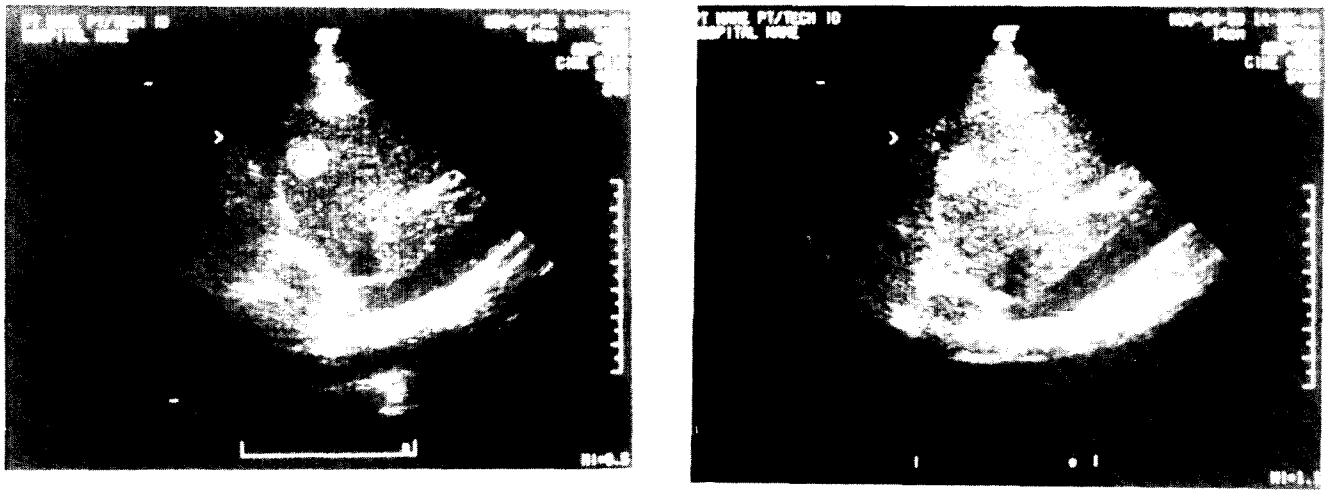

Figure 8: images of liver of subject with hemangioma. The contrast between this tumor and the surrounding tissue is enhanced with the 1.5D array (right image) compared with the 1D array (left).

References

[1] M. O'Donnell, "Efficient parallel receive beam forming for phased array imaging using phase rotation," *Proc. 1990 IEEE Ultrasonics Symposium,* 1495-1498.

[2] C.M.W. Daft, L.S. Smith and M. O'Donnell, "Beam profiles and images from two-dimensional arrays," *Proc. 1990 IEEE Ultrasonics Symposium,* 1053-1056.

[3] R.E. Davidsen and S.W. Smith, "Sparse geometries for two-dimensional array transducers in volumetric imaging," *Proc. 1993 IEEE Ultrasonics Symposium,* 1091-1094.